Simultaneous measurement of temperature and refractive index using an exposed core microstructured optical fiber

Xuegang Li, Linh V. Nguyen, Martin Becker, Heike Ebendorff-Heidepriem, Dinh Pham, and Stephen C. Warren-Smith

***Abstract*—We have demonstrated a novel scheme for simultaneous measurement of temperature and refractive index by using an exposed core microstructured optical fiber (ECF). The ECF allows for high sensitivity to refractive index due to the small exposed-core, while being supported by a standard fiber diameter cladding making it robust compared to optical micro-fibers. The sensor combines a fiber Bragg grating (FBG) inscribed into the core of the ECF and a multimode Mach-Zehnder interferometer (MZI). Both the FBG and MZI are sensitive to refractive index (RI) and temperature through a combination of direct access to the evanescent field via the exposed-core, the thermo-optic effect and thermal expansion. The FBG and MZI respond differently to changes in temperature and RI, thus allowing for the simultaneous measurement of these parameters. In our experiment RI sensitivities of 5.85 nm/RIU and 794 nm/RIU, and temperature sensitivities of 8.72 pm/°C and -57.9 pm/°C, were obtained for the FBG and MZI respectively. We demonstrate that a transfer matrix approach can be used to simultaneously measure both parameters, solving the problem of temperature sensitivity of RI sensors due to the high thermo-optic coefficient of aqueous samples.**

***Index Terms*—Optical interferometry, optical fibers, optical sensors.**

I. Introduction

VARIOUS optical fiber refractive index (RI) sensors have been proposed and developed due to their advantageous properties, such as small size, high sensitivity, bio-compatibility, suitability for remote operation and in harsh conditions, and immunity to electromagnetic interference. A series of techniques for RI sensing with optical fibers have been demonstrated, such as fiber Bragg-gratings [1, 2], Mach-Zehnder interferometers (MZIs) [3], Fabry-Perot interferometers (FPIs) [4], Sagnac interferometers [5], and Surface Plasmon Resonance (SPR) [6]. However, a common drawback of RI sensors is that they are also sensitive to temperature. In particular, water has a relatively large thermo-optic coefficient, thus RI based biochemical sensors require either highly stable temperature environments to operate accurately or the ability to compensate for the temperature effect via simultaneous measurement of RI and temperature. Therefore, several methods have been designed to achieve the simultaneous measurement of RI and temperature.

Several hybrid interferometers have been proposed, such as two different Mach–Zehnder interferometers [7], a Mach–Zehnder interferometer combined with a Fabry–Perot interferometer [8, 9], and a Sagnac interferometer combined with a Mach–Zehnder interferometer [10, 11]. Multimode interferometers with standard diameter fibers have been demonstrated for the simultaneous measurement of RI and temperature by utilizing different order modes have different sensitivities to the external RI and temperature, and other parameters [12-14]. However, such interferometers suffer low RI sensitivity and thus it is common to taper or etch the fiber to produce an optical microfibers, which are typically fragile and susceptible to mechanical effects such as bending. For example, a dual long-period grating (LPG) sensor for simultaneous measurement of the RI and temperature was thinned via etching to achieve simultaneous refractive index and temperature sensing. [15]. A dual MZI by inserting a section of multimode microfiber (with 11.24μm diameter) in the sensing arm of a MZI setup was demonstrated, providing simultaneous measurement of RI and temperature with high sensitivities [16].

Stephen C. Warren-Smith is funded by a Ramsay Fellowship provided by the University of Adelaide. This work was performed, in part, at the Optofab node of the Australian National Fabrication Facility utilizing Commonwealth and SA State Government funding. This work was supported by the Australian Research Council (ARC) Centre for Nanoscale BioPhotonics (CE14010003) and an ARC Linkage Project (LP150100657). Xuegang Li gratefully acknowledges financial support from the China Scholarship Council. This work was supported in part by the Fundamental Research Funds for the Central Universities under Grant N160406004. The authors acknowledge Evan Johnson and Alastair Dowler for their contribution to the fiber fabrication.

Xuegang Li is with College of Information Science and Engineering, Northeastern University, Shenyang 110819, China, and also with Institute for Photonics and Advanced Sensing (IPAS) and School of Physical Sciences, The University of Adelaide, Adelaide, South Australia 5005, Australia (e-mail: lixuegang@stumail.neu.edu.cn).

Linh V. Nguyen and Dinh Pham are with Institute for Photonics and Advanced Sensing (IPAS) and School of Physical Sciences, The University of Adelaide, Adelaide, South Australia 5005, Australia (e-mail: linhnguyen.research@gmail.com, dinh.pham@adelaide.edu.au).

Martin Becker is with Leibniz Institute of Photonic Technology, Albert-Einstein-Str. 9, 07745 Jena, Germany. (martin.becker@leibniz-ipht.de).

Stephen C. Warren-Smith and Heike Ebendorff-Heidepriem are with Institute for Photonics and Advanced Sensing (IPAS) and School of Physical Sciences, The University of Adelaide, Adelaide, South Australia 5005, Australia, and also with ARC Centre of Excellence for Nanoscale BioPhotonics (CNBP), The University of Adelaide, Adelaide, South Australia 5005, Australia (e-mail: stephen.warrensmith@adelaide.edu.au, heike.ebendorff@adelaide.edu.au).

However etched or tapered fiber can easily be damaged, particularly if made micron-scaled to achieve high refractive index sensitivity.

Alternatively, a dual-channel SPR-based optical fiber sensor for simultaneous monitoring of temperature and refractive index has been proposed and demonstrated. The sensor consisted of a multimode - single mode - multimode structured fiber with a double-sided gold layer where half of the gold-coated SMF section was covered with a high thermo-optic coefficient polymer. Simultaneous measurement was achieved by monitoring two independent SPR resonance dips [17]. However, this method relies on metal films and polymers that can suffer instability issues and high loss in an optical fiber configuration.

Various optical fiber temperature sensors have also been proposed and developed [2, 18-21]. Fiber Bragg gratings (FBGs) are well known for their use in optic fiber temperature sensing, though when in a conventional step-index fiber they are not sensitive to refractive index without further post-processing such as tapering or etching. FBGs can be combined serially with interferometric RI sensors [22, 23], but this results in the refractive index and temperature sensing being spatially separated and again requires a means of fabricating a sensitive interferometric RI sensor.

We have previously fabricated FBGs in exposed-core microstructured optical fibers, which were demonstrated to respond to both refractive index and temperature in a configuration more robust than a tapered fiber [24]. While it is in principle possible to measure both parameters simultaneously using the higher order mode FBG reflections, the sensor had relatively poor sensitivity to RI the order of only 1-5 nm/RIU [1, 24]. We have since shown that interferometric based exposed-core fiber sensors can offer high RI sensitivity [25, 26], such as 667 nm/RIU in a multimode Mach-Zehnder configuration [25].

In this work, we have designed and demonstrated a novel scheme for co-located simultaneous and high sensitivity measurement of temperature and external RI by combining the RI sensitivity of an interferometric-based ECF sensor with the temperature sensitivity of an FBG (ECF-FBG).

II. Operating Principle

Fig. 1(a) shows a schematic diagram of the ECF-FBG sensor. It contains a Mach-Zehnder interferometer, fabricated by splicing a section of few-mode ECF between two single mode fibers, and an FBG that is inscribed into the core of the ECF. Fig. 1(b) shows a cross-sectional image of the ECF, which has the core exposed to the external environment on one side. The high numerical aperture of the ECF allows for propagation of a number of higher order modes. Thus, when the light from a broad-band source enters the ECF from the lead-in single mode fiber, higher order modes are excited and propagate along the ECF core. Mach-Zehnder interference occurs between the different order modes due to different propagation constants. Meanwhile, a narrow wavelength band is reflected by the FBG.

For the Mach–Zehnder interferometer, the transmission spectrum can be analyzed using a simple two-mode interference

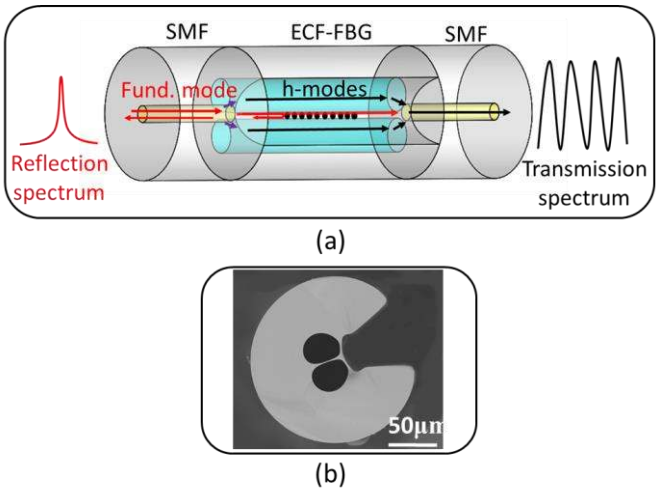

Fig. 1. (a) Schematic diagram of an ECF-FBG Mach–Zehnder interferometer. (b) Scanning electron microscope (SEM) image of the exposed-core microstructured optical fiber. *h-modes* refers to higher order modes.

model,

$$I_{out} = I_i + I_j + 2\sqrt{I_i I_j}\cos(\varphi), \quad (1)$$

where I_i and I_j are light intensities of two different modes, and φ is the phase difference between them. Assuming negligible dispersion over the measured wavelength range, the phase difference, φ, can be expressed as,

$$\varphi = \frac{2\pi L_{ECF}}{\lambda}\Delta n_{eff}, \quad (2)$$

where λ is the free space wavelength, L_{ECF} is the length of the ECF, and Δn_{eff} is the effective index difference between the i^{th} and j^{th} modes. Δn_{eff} can be expressed as,

$$\Delta n_{eff} = n_{eff}^{i}(\lambda, n_{ext}, T) - n_{eff}^{j}(\lambda, n_{ext}, T), \quad (3)$$

where n_{eff}^{i} and n_{eff}^{j} are the effective indexes of the i^{th} and j^{th} modes, which are affected by ambient temperature, T, and external RI, n_{ext}, due to the thermo-optic effect and the exposed core design of the fiber allowing direct access to the evanescent field. The effective indexes changes of the different modes are different when the external environment changes. Thus Δn_{eff} will change due to changes in the external environment. With a change in the external RI or temperature, the changes in phase, $\delta\varphi$, caused by the change of Δn_{eff}, ($\delta\Delta n_{eff}$), can be expressed as,

$$\delta\varphi = \frac{2\pi L_{ECF}}{\lambda}\delta(\Delta n_{eff}). \quad (4)$$

Note that the change of the ECF length with temperature is very small compared to the thermo-optic coefficient of water, thus the change in phase due to thermal expansion is negligible.

Further, the wavelength shift of the interference fringes can be expressed as

$$\delta\lambda = \frac{\lambda^2}{2\pi\Delta n_{eff} L_{ECF}}\delta\varphi = \frac{FSR}{2\pi}\delta\varphi\,, \tag{5}$$

where FSR is the free spectral range.

The values of phase change ($\delta\varphi$) and FSR can be obtained by applying a fast Fourier transform (FFT) on the transmission spectra. Note that the FSR (interference period) of the wavelength spectrum is a function of wavelength, while it is independent of wavelength/frequency in the optical frequency spectrum. Thus, for our experimental results that follow we first converted the wavelength on the x-axis to optical frequency before applying an FFT.

FFT techniques are widely used for de-multiplexing interference spectra [25, 26], which is more precise than other methods of tracking interference spectrum shifts, such as peak tracking or function fitting [27]. The value of the phase (φ) is taken from the complex value at the FFT peak. The value of FSR is taken from the x-coordinate value of the FFT peak. The phase change ($\delta\varphi$) with respect to changes in the ambient medium are then determined by subtracting the phase value of an initial spectrum. Finally, the wavelength change of the interference spectrum can be calculated using (5).

For first order FBG, the reflected wavelength, λ_B, known as the Bragg wavelength, is defined by the relationship [24],

$$\lambda_B = [n_{eff,f}(\lambda, n_{ext}, T) + n_{eff,b}(\lambda, n_{ext}, T)]\Lambda(T)\,, \tag{6}$$

where $n_{eff,f}$ and $n_{eff,b}$ are the forward and backward effective indices of any two modes in the fiber core, respectively. The Bragg wavelength is affected by ambient temperature and external RI, while the grating period, Λ, is sensitive temperature via thermal expansion. That is, the Bragg wavelength changes with different external RI and temperature. Note that there will be several FBG peaks in the reflection spectrum due to the higher order modes present in the ECF, as previously observed in both ECF [1, 24] and similar suspended-core microstructured optical fiber [19, 28].

Thus, both the Mach–Zehnder interferometer and FBG are sensitive to external RI and temperature, and can thus achieve the simultaneous measurement of temperature and external RI by simultaneously monitoring the wavelength shifts of the FBG reflection spectrum and the Mach–Zehnder interference transmission spectrum. The use of two wavelength-based (intensity independent) measurement techniques also aids in forming a stable and repeatable sensor as the sensor will be minimally sensitive to changes in the fabrication process such as fibre loss, cleaving and splicing.

III. Experimental Setup and Results

A. Experimental setup and spectral analysis

Fig. 2 shows a schematic diagram of the proposed sensing system using the ECF-FBG Mach–Zehnder interferometer.

First, an 11 cm length of ECF was fusion-spliced between two single mode fibers using an arc splicer (Fujikura FSM-100P) with the same splicing conditions previously reported in [1]. The ECF was fabricated by using a two-step technique. Briefly, a preform was first fabricated by using ultrasonic drilling and cutting. The preform was then drawn into fiber using a 6 m tall drawing tower with a graphite resistance furnace and positive internal pressure. Further details on the fabrication technology of the ECF has been described in [1, 29]. A first-order FBG was then written into the core of the ECF using two beam interference and a 5 minute exposure to a deep UV (267 nm) femtosecond laser source, as previously described [30]. Two channels of an FBG interrogator (National Instruments PXIe-4844), which had a resolution of 4 pm, were used to measure both reflection and transmission spectra of our sensor.

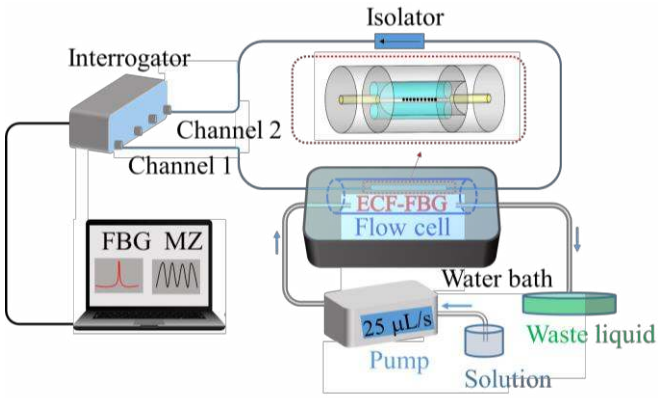

Fig. 2. Schematic diagram of the proposed sensor system.

The ECF-FBG was packaged within a silica capillary flow cell (inner diameter of 650 μm) and then placed into a temperature controlled water bath (Memmert Waterbath WNB 7) with a resolution of 0.1°C to achieve simultaneous change of the external RI and temperature, as shown in Fig. 2. RI was changed by flowing NaCl solutions of different mass concentration through the flow cell via a pump (LongerPump BT100-1F) and the temperature was changed by varying the water bath temperature.

Four example reflection spectra and transmission spectra are shown in Fig. 3(a) and 3(b), respectively. Fig. 3(c) shows a FFT of the first interference spectrum shown in Fig. 3(b). Multiple peaks are observed, which indicate that at least three modes were strongly excited in the ECF. In our work, we selected the peak of 0.3750 nm^{-1} as the Mach-Zehnder interference sensing peak and the highest FBG peak at 1542 nm in Fig. 3(a) as the FBG sensing peak.

B. Simultaneous measurement of temperature and refractive index

The reflection and transmission spectra were recorded as the

flow cell was filled with solutions of sodium chloride in DI water (0-0.9% with 0.3% steps), at different ambient temperatures (24-30°C with 2°C steps), with four example spectra shown in Figs. 3(a) and 3(b), respectively.

The value of the FBG wavelength shift was tracked using a Gaussian fitting method. Meanwhile, the wavelength change of the Mach-Zehnder interference spectrum can be calculated from (5), where the values of phase change ($\Delta\varphi$) and FSR were obtained by applying an FFT on the transmission spectra. Fig. 4 shows that the FBG peak shifts to longer wavelengths with increasing concentration and temperature, while the Mach-

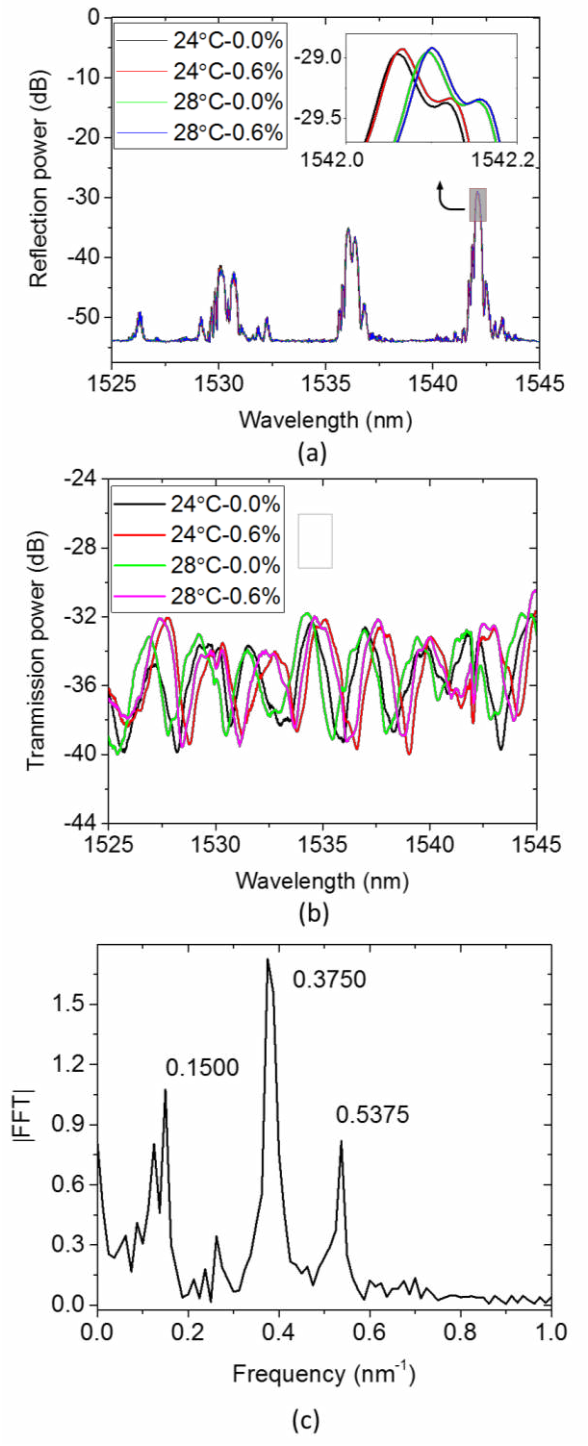

Fig. 3. (a) Reflection spectra and (b) transmission spectra of the sensor with different external RI and ambient temperature. (c) FFT spectrum of the first interference spectrum shown in Fig. 3(b) (black curve).

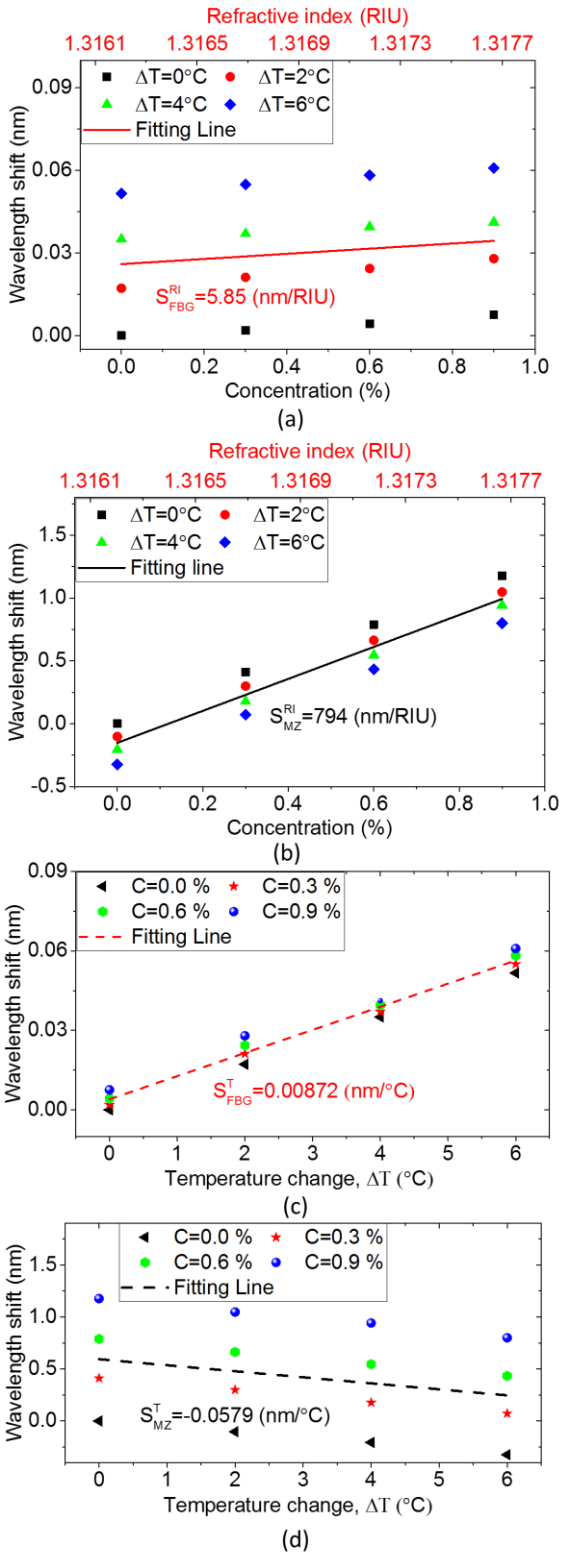

Fig. 4. Wavelength shifts of the (a) FBG peak and (b) MZI transmission spectrum with different concentrations in different temperatures. Wavelength shifts of the (c) FBG peak and (d) MZI transmission spectrum with different temperatures in different concentrations.

Zehnder interference spectra shifts to longer wavelengths with increasing concentration and decreasing temperature. Further, the concentration values were converted to RI by using the following equation,

$$n = -0.08C^3 + 0.074C^2 + 0.162C + 1.3162, \quad (7)$$

where n is the RI of the NaCl solutions and C is the concentration [31]. From Figs. 4(a) and 4(b), the concentration sensitivities of the FBG, $S_{\mathrm{FBG}}^{\mathrm{C}}$, and Mach-Zehnder interferometer, $S_{\mathrm{MZ}}^{\mathrm{C}}$, are estimated to be 9.37 pm/% and 1.273 nm/%, respectively. Converting to RI sensitivities [31], the sensitivities, $S_{\mathrm{FBG}}^{\mathrm{RI}}$ and $S_{\mathrm{MZ}}^{\mathrm{RI}}$, are 5.85 nm/RIU and 794 nm/RIU, respectively. The temperature sensitivities of the FBG, $S_{\mathrm{FBG}}^{\mathrm{T}}$, and Mach-Zehnder interferometer, $S_{\mathrm{MZ}}^{\mathrm{T}}$, are 8.72 pm/°C and -57.9 pm/°C, respectively, as shown in Figs. 4(c) and 4(d). The temperature sensitivity of the FBG is approximately equal to values previously reported [24]. Table 1 shows a summary of standard diameter (≥125 μm) optical fiber interferometric and/or grating sensors for simultaneous measurement of RI and temperature. It can be seen from Table 1 that our sensor shows a significantly higher RI sensitivity compared with LPGs, FBG and similar interferometers without post-processing such as tapering and etching.

Table 1 Summary of optical fiber sensors with standard diameter fiber (≥ 125 μm) for simultaneous measurement of RI and temperature.

Category	Sensing theory	Temperature Sensitivity (pm/°C)	RI sensitivity (nm/RIU)	Reference
Hybrid interferometers	Different configurations of interferometers have different sensitivities to RI and temperature.	139, 454, 27.5. 1700	101, 179, 108, 219	[7-10]
MZ mode interferometers	Different order modes have different sensitivities to RI and temperature.	52.2, 59.0, 131	37.9, 86.7, 111	[12-14]
FBGs combined with core-offset MZ interferometer	FBGs were used to measure temperature, while the interferometric sensors were used for measuring RI.	46.2	13.8	[23]
FBG in a multimode ECF	Different order mode FBG reflections have different sensitivities to RI and temperature.	> 10	1.1	[24]
FBG combined with ECF interferometer	**The FBG and MZ interferometer have different sensitivities to RI and temperature.**	**-57.9**	**794**	**This paper**

Based on external RI and temperature sensitivities obtained in Fig. 4, simultaneous measurement can be achieved by using the following matrix,

$$\begin{bmatrix} \Delta C \\ \Delta T \end{bmatrix} = \begin{bmatrix} S_{\mathrm{FBG}}^{\mathrm{RI}} & S_{\mathrm{FBG}}^{\mathrm{T}} \\ S_{\mathrm{MZ}}^{\mathrm{RI}} & S_{\mathrm{MZ}}^{\mathrm{T}} \end{bmatrix}^{-1} \begin{bmatrix} \Delta\lambda_{\mathrm{FBG}} \\ \Delta\lambda_{\mathrm{MZ}} \end{bmatrix}. \quad (8)$$

Further, we can get the matrix based on calibrated (experimentally measured) values,

$$\begin{bmatrix} \Delta C \\ \Delta T \end{bmatrix} = \begin{bmatrix} 5.85 & 0.00872 \\ 794 & -0.0579 \end{bmatrix}^{-1} \begin{bmatrix} \Delta\lambda_{\mathrm{FBG}} \\ \Delta\lambda_{\mathrm{MZ}} \end{bmatrix}, \quad (9)$$

where $\Delta\lambda_{\mathrm{FBG}}$ and $\Delta\lambda_{\mathrm{MZ}}$ are the wavelength shifts of the FBG peak and Mach-Zehnder interference spectrum, respectively. Using (9) we calculated the measured concentration and temperature. The measured values, target values and the measured differences between the measured values and target values were shown in Fig.5. It can be seen from Fig.5 that the measured values are in good agreement with a maximum measured difference between the target values and the sensor values of 0.0296% (4.81×10^{-5} RIU) and 0.214°C, for concentration and temperature, respectively. Thus, we can accurately obtain the unknown external RI and temperature variations by simultaneously monitoring the wavelength shifts of the FBG peak, and Mach-Zehnder interference spectrum and using (9).

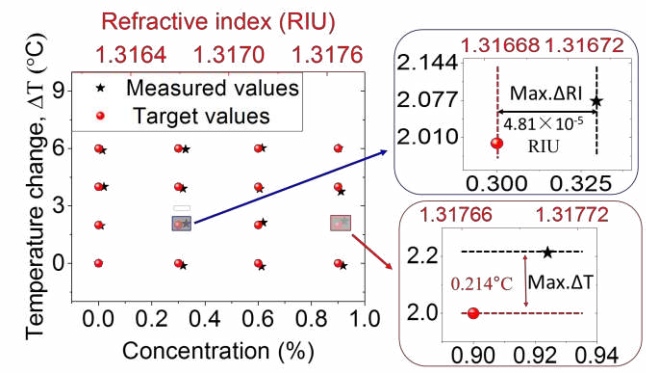

Fig. 5. Measured values of external RI and temperature compared with target values. "Max. ΔT" and "Max. ΔC" are the maximum measured differences between the target and measured values.

IV. Conclusion

A novel scheme for simultaneous measurement of refractive index and temperature using an ECF-FBG has been designed and demonstrated. By tracking the wavelength shifts of the FBG peak and Mach-Zehnder interference spectrum, RI sensitivities of 5.85 nm/RIU and 794 nm/RIU, as well as temperature sensitivities of 8.72 pm/°C and -57.9 pm/°C, can be achieved. The RI sensitivity of the proposed sensor is two orders of magnitude higher than the FBG sensor in [24]. When used for simultaneous measurement the measured values are in good agreement with the prepared values with a maximum measured RI difference of 4.81×10^{-5} RIU, and a maximum measured temperature difference of 0.214°C. The proposed sensor provides a higher RI sensitivity compared with other FBGs or interferometers without post-processing such as tapering and etching, while solving the issue of temperature sensitivity when measuring aqueous samples. The sensor has potential application in temperature-compensated chemical–biochemical sensing applications, owing to its advantages of real-time measurement, bio-compatibility and small size.

References

[1] S. C. Warren-Smith, R. Kostecki, L. V. Nguyen, and T. M. Monro, "Fabrication, splicing, Bragg grating writing, and polyelectrolyte functionalization of exposed-core microstructured optical fibers," *Optics Express,* vol. 22, no. 24, pp. 29493-29504, 2014.

[2] D. A. Pereira, O. Frazao, and J. L. Santos, "Fiber Bragg grating sensing system for simultaneous measurement of salinity and temperature," *Optical Engineering,* vol. 43, no. 2, pp. 299-305, 2004.

[3] W. J. Yu, T. T. Lang, J. C. Bian, and W. Kong, "Label-free fiber optic biosensor based on thin-core modal interferometer," *Sensors and Actuators B-Chemical,* vol. 228, pp. 322-329, 2016.

[4] Y. Zhang, H. Shibru, K. L. Cooper, and A. B. Wang, "Miniature fiber-optic multicavity Fabry-Perot interferometric biosensor," *Optics Letters,* vol. 30, no. 9, pp. 1021-1023, 2005.

[5] S. Gao, L. P. Sun, J. Li, L. Jin, Y. Ran, Y. Y. Huang, and B. O. Guan, "High-sensitivity DNA biosensor based on microfiber Sagnac interferometer," *Optics Express,* vol. 25, no. 12, pp. 13305-13313, 2017.

[6] J. D. Lu, T. Van Stappen, D. Spasic, F. Delport, S. Vermeire, A. Gils, and J. Lammertyn, "Fiber optic-SPR platform for fast and sensitive infliximab detection in serum of inflammatory bowel disease patients," *Biosensors & Bioelectronics,* vol. 79, pp. 173-179, 2016.

[7] Z. Tong, J. Su, Y. Cao, and W. Zhang, "Simultaneous measurement based on composite interference structure," *IEEE Photonics Technology Letters,* vol. 26, no. 13, pp. 1310-1313, 2014.

[8] Y. Zhao, X.-G. Li, L. Cai, and Y.-N. Zhang, "Measurement of RI and temperature using composite interferometer with hollow-core fiber and photonic crystal fiber," *IEEE Transactions on Instrumentation and Measurement,* vol. 65, no. 11, pp. 2631-2636, 2016.

[9] X.-G. Li, Y. Zhao, L. Cai, and Q. Wang, "Simultaneous measurement of RI and temperature based on a composite interferometer," *IEEE Photonics Technology Letters,* vol. 28, no. 17, pp. 1839-1842, 2016.

[10] Y. Zhao, X. Liu, R.-q. Lv, and Q. Wang, "Simultaneous measurement of RI and temperature based on the combination of Sagnac loop mirror and balloon-like interferometer," *Sensors and Actuators B: Chemical,* vol. 243, pp. 800-805, 2017.

[11] K. Naeem, B. H. Kim, B. Kim, and Y. Chung, "Simultaneous multi-parameter measurement using Sagnac loop hybrid interferometer based on a highly birefringent photonic crystal fiber with two asymmetric cores," *Optics Express,* vol. 23, no. 3, pp. 3589-601, 2015.

[12] R. Xiong, H. Meng, Q. Yao, B. Huang, Y. Liu, H. Xue, C. Tan, and X. Huang, "Simultaneous measurement of refractive index and temperature based on modal interference," *IEEE Sensors* Journal, vol. 14, no. 8, pp. 2524-2528, 2014.

[13] H. Wang, H. Meng, R. Xiong, Q. Wang, B. Huang, X. Zhang, W. Yu, C. Tan, and X. Huang, "Simultaneous measurement of refractive index and temperature based on asymmetric structures modal interference," *Optics Communications*, vol. 364, pp. 191-194, 2016.

[14] J. Su, Z. Tong, Y. Cao, and P. Luan, "Double-parameters optical fiber sensor based on spherical structure and multimode fiber," *IEEE Photonics Technology Letters,* vol. 27, no. 4, pp. 427-430, 2015.

[15] J. Yan, A. P. Zhang, L.-Y. Shao, J.-F. Ding, and S. He, "Simultaneous measurement of refractive index and temperature by using dual long-period gratings with an etching process," *IEEE Sensors Journal,* vol. 7, no. 9, pp. 1360-1361, 2007.

[16] H. Luo, Q. Sun, Z. Xu, D. Liu, and L. Zhang, "Simultaneous measurement of refractive index and temperature using multimode microfiber-based dual Mach–Zehnder interferometer," *Optics Letters,* vol. 39, no. 13, pp. 4049-4052, 2014.

[17] J. S. Velázquez-González, D. Monzón-Hernández, D. Moreno-Hernández, F. Martínez-Piñón, and I. Hernández-Romano, "Simultaneous measurement of refractive index

and temperature using a SPR-based fiber optic sensor," *Sensors and Actuators B: Chemical,* vol. 242, pp. 912-920, 2017.

[18] J. H. Liou, and C. P. Yu, "All-fiber Mach-Zehnder interferometer based on two liquid infiltrations in a photonic crystal fiber," *Optics Express,* vol. 23, no. 5, pp. 6946-51, 2015.

[19] S. C. Warren-Smith, L. V. Nguyen, C. Lang, H. Ebendorff-Heidepriem, and T. M. Monro, "Temperature sensing up to 1300°C using suspended-core microstructured optical fibers," *Optics Express,* vol. 24, no. 4, pp. 3714-3719, 2016.

[20] F. Favero, M. Becker, R. Spittel, M. Rothhardt, J. Kobelke, and H. Bartelt, "Micro-structured fiber interferometer as sensitive temperature sensor," *Photonic Sensors,* vol. 3, no. 3, pp. 208-213, 2013.

[21] Y. Zhao, F. Xia, H.-F. Hu, and C. Du, "A ring-core optical fiber sensor with asymmetric LPG for highly sensitive temperature measurement," *IEEE Transactions on Instrumentation and Measurement,* vol. 66, no. 12, pp. 3378-3386, 2017.

[22] M. Wang, D. N. Wang, M. Yang, J. Cheng, and J. Li, "In-line Mach-Zehnder Interferometer and FBG with Pd film for simultaneous hydrogen and temperature detection," *Sensors and Actuators B: Chemical,* vol. 202, pp. 893-896, 2014.

[23] Q. Yao, H. Meng, W. Wang, H. Xue, R. Xiong, B. Huang, C. Tan, and X. Huang, "Simultaneous measurement of refractive index and temperature based on a core-offset Mach–Zehnder interferometer combined with a fiber Bragg grating," *Sensors and Actuators A: Physical,* vol. 209, pp. 73-77, 2014.

[24] S. C. Warren-Smith, and T. M. Monro, "Exposed core microstructured optical fiber Bragg gratings: refractive index sensing," *Optics Express,* vol. 22, no. 2, pp. 1480-1489, 2014.

[25] L. V. Nguyen, K. Hill, S. Warren-Smith, and T. Monro, "Interferometric-type optical biosensor based on exposed core microstructured optical fiber," *Sensors and Actuators B-Chemical,* vol. 221, pp. 320-327, 2015.

[26] X. Li, L. V. Nguyen, Y. Zhao, H. Ebendorff-Heidepriem, and S. C. Warren-Smith, "High-sensitivity Sagnac-interferometer biosensor based on exposed core microstructured optical fiber," *Sensors and Actuators B: Chemical*, vol. 269, pp. 103-109, 2018.

[27] J. Silverstone, S. McFarlane, C. Manchee, and A. Meldrum, "Ultimate resolution for refractometric sensing with whispering gallery mode microcavities," *Optics Express,* vol. 20, no. 8, pp. 8284-8295, 2012.

[28] L. A. Fernandes, M. Becker, O. Frazao, K. Schuster, J. Kobelke, M. Rothhardt, H. Bartelt, J. L. Santos, and P. V. Marques, "Temperature and strain sensing with femtosecond laser written Bragg gratings in defect and nondefect suspended-silica-core fibers," *IEEE Photonics Technology Letters,* vol. 24, no. 5, pp. 554, 2012.

[29] R. Kostecki, H. Ebendorff-Heidepriem, C. Davis, G. McAdam, S. C. Warren-Smith, and T. M. Monro, "Silica exposed-core microstructured optical fibers," *Optical Materials Express,* vol. 2, no. 11, pp. 1538-1547, 2012.

[30] M. Becker, L. Fernandes, M. Rothhardt, S. Bruckner, K. Schuster, J. Kobelke, O. Frazao, H. Bartelt, and P. V. Marques, "Inscription of fiber Bragg grating arrays in pure silica suspended core fibers," *IEEE Photonics Technology Letters,* vol. 21, no. 19, pp. 1453-1455, 2009.

[31] J. E. Saunders, C. Sanders, H. Chen, and H.-P. Loock, "Refractive indices of common solvents and solutions at 1550 nm," *Applied Optics,* vol. 55, no. 4, pp. 947-953, 2016.

Xuegang Li was born in Hebei, China, in December 1991. He received his B. A. degree in the College of Information Science and Engineering from the Northeastern University, China, in 2014. He is now a visiting PhD student of the University of Adelaide. His research interests are photonic crystal fiber sensors, optical modal interference sensors, in-fiber interferometer and its sensing applications. He has authored and co-authored more than ten scientific papers.

Linh V. Nguyen obtained a PhD in Information and Communications from Gwangju Institute of Science and Technology (GIST), South Korea, in 2009. His graduate works focused on the development of fiber-optics devices for applications in fiber sensor, fiber laser and all-optical signal processing. In 2010 he moved to Edith Cowan University (ECU) in Western Australia to work on the development of fiber-optics sensors for applications in desalination and seawater-related industries. He joined the Institute for Photonics & Advanced Sensing (IPAS), School of Physical Sciences at the University of Adelaide in 2011 as an Australian Research Council (ARC) Super Science Fellow leading a project toward development of rapid protein sensing and blood typing platform at crime scenes and subsequently on a project developing of tools for in-field surveillance of pathogens in a Researcher/Chief Investigator capacity. Currently he is working on development of densely multiplexed high temperature sensors for industrial applications.

Heike Ebendorff-Heidepriem received the Ph.D. degree in chemistry from the University of Jena, Germany, in 1994. She received the Weyl International Glass Science Award and the prestigious Marie Curie Individual Fellowship of the European Union in 2001. During 2001-2004 she was with the Optoelectronics Research Centre at the University of Southampton, UK. Since 2005, she has been with the University of Adelaide, Australia. Currently, she leads the Fibers and Photonics Materials research group and is the Deputy Director of the Institute for Photonics and Advanced Sensing. She is also the Deputy Director of the Optofab node of the Australian National Fabrication Facility (ANFF) and Senior Investigator of the ARC Centre of Excellence for Nanoscale BioPhotonics (CNBP). Her research focuses on the development of novel optical glasses, specialty optical fibers, hybrid glasses and fibers, surface functionalization and sensing approaches.

Dinh Pham was born in Ho Chi Minh city, Vietnam. He received B.A degree in The University of Science, Vietnam National University. He is a research assistant in the institute for Photonics and Advanced Sensing - University of Adelaide. His research interest is photonics crystal fiber sensors. Currently he is working on development of densely multiplexed high temperature sensors for industrial applications.

Stephen C. Warren-Smith completed his PhD in 2011 at the University of Adelaide, Australia, on the topic of microstructured optical fiber chemical sensing. He was then employed from 2011 to 2014 as an Australian Research Council (ARC) Super Science Fellow at the Institute for Photonics and Advanced Sensing and the School of Chemistry and Physics at the University of Adelaide, working on optical fiber biosensing for women's health applications. In 2015 and 2016 he worked as a European Union Marie Curie International Incoming Fellow at the Leibniz Institute of Photonic Technology, Jena, Germany, on a project investigating the micro/nano-structuring of optical fibers for sensing. Since October 2016 he is with the University of Adelaide as a Ramsay Fellow.